Electronic Supplementary Information for

Density Controlled Oil Uptake and Beyond: From Carbon Nanotube to Graphene Nanoribbon Aerogels

By Liang Chen, Ran Du, Jin Zhang* and Tao Yi*

[*] Prof. T. Yi, L. Chen
Department of Chemistry and Collaborative Innovation Center of Chemistry for Energy Materials, Fudan University, 220 Handan Road, Shanghai 200433, P.R. China.
E-mail: yitao@fudan.edu.cn

[*] Prof. J. Zhang, R. Du
Center for Nanochemistry, Beijing National Laboratory for Molecular Sciences, Key Laboratory for the Physics and Chemistry of Nanodevices, State Key Laboratory for Structural Chemistry of Unstable and Stable Species, College of Chemistry and Molecular Engineering, Peking University, Beijing 100871, P.R. China.
E-mail: jinzhang@pku.edu.cn

Part I: Experimental section:

Reagents and Materials

Multi-wall carbon nanotubes (MWNTs) with average length of 10 μm and average diameter of 11 nm were obtained from CNano Technology company Ltd. Graphene oxide (GO) were prepared according to methods reported elsewhere.[s1] Pyrrole (Py), and other reagents were purchased from commercial suppliers (Alfa-Aesar, TCI and Aladdin Chemistry Co., Ltd.). All reagents were used without further purification.

Preparation of oxidized nano-carbon precursors

The oxidized MWNTs (ox-MWNTs) were prepared by using a modified Hummer's method, GONRs and partially unzipped CNTs (CNTs@GONRs) were prepared by longitudinally unzipping MWNTs under acid condition. Details can be found elsewhere. [s2-s5]

Preparation of aerogels

Oxidized nano-carbon precursors in water (1~12 mg mL^{-1}) was mixed with pyrrole (0~30 vol%) in a Taflon vessel. The mixture was subjected to a stainless steel hydrothermal reactor to conduct hydrothermal reaction at 180 °C for 12 h, followed by naturally cooling to room temperature. Then the free-standing hydrogels can be obtained.

The as-prepared hydrogels were washed with deionized water for twice and exchanged the solvents with tertiary butanol for 4 times. Then the wet gels were flash-frozen by liquid nitrogen and freeze-dried at ~1 Pa for at least 24 h to create the corresponding aerogels.

Thermal treatment of aerogels were done at high temperature (500, 750 or 1030 °C) for 3 hours under the protection of argon.

Part II: Characterizations

Electron Microscopy

Scanning electron microscopy (SEM) and energy dispersive X-Ray spectroscopy (EDX) were conducted on a Hitachi S-4800 field-emission-gun scanning electron microscope. The samples were prepared by directly putting aerogels on the conductive tape.

High-resolution transmission electron microscopy (HRTEM) analysis was carried out by Tecnai F20 at 200 kV. The samples were prepared by dispersing aerogels in ethanol with assistance of ultrasonication, followed by dropping the gel solution on carbon coated copper grids and drying at ambient temperature.

XRD Spectroscopy

X-ray powder diffraction patterns (XRD) were measured with a X’Pert Pro (Philips) diffractometer with monochromatic Cu Kα1 radiation (λ = 1.5406 Å) at 40 kV and 40 mA. The diffraction patterns were optimized with a step length of 0.0167° (2θ) over an angular range 5-50° (2θ) with a scanning speed of 0.025°/s.

Contact Angle Measurement

Contact angle measurement was directly conducted on the aerogel at room temperature. The data was collected by OCA20 (Dataphysics).

The Porosity and Pore volume Calculation

The porosity of aerogels can be calculated as follows,[s6, s7]

$$\eta = 1 - \frac{\rho_{app}}{\rho_c}$$

Where the ρ_{app}, ρ_c represented the apparent aerogel density and the density of aerogels network, respectively. In our case, the ρ_c was the bulk density of MWNTs or graphite. Since the density of MWNTs (~2.1 g cm^{-3}) and GNRs (2.2 g cm^{-3}) were similar to that of graphite (2.2 g cm^{-3}), [s8, s9] the porosities of all carbon-based aerogels in our cases are linearly correlated to the apparent density of aerogels.

For the pore volume (V_a) of all size pores inside aerogels, the value can be calculated as follows.

$$V_a = V_{tot} - V_c = \frac{1}{\rho_{app}} - \frac{1}{\rho_c}$$

Where V_a, V_{tot}, and V_c represented the pore volume, the total volume of 1 g aerogel, and the volume occupied 1 g aerogel network, respectively.

Oil uptake Measurement

Typically, a piece of aerogel (ca. 2 mg) was dropped into organic solvent or oil for several hours to realize saturated adsorption, although the majority adsorption could be finished within several seconds. Then the weight gain (%) of aerogel was calculated by

$$q_{\mathrm{m}} = 100^*(m\text{-}m_0)/m_0$$

Where m_0 and m represent the mass of aerogel before and after adsorption, respectively.

The regeneration of aerogel could be achieved by either burning the gel in the air or heating the adsorbed gel at 60 °C for a period of time.

Densitometer

Assuming that the aerogel could be fully saturated by all kinds of solution because of their amphiphilic property, and its density could be regarded to zero owing to their very low density compared to that of solvents. Then the aerogel could be visualized as a massless container capable of accommodating different liquid.

On this occasion, when the aerogel was saturated in an unknown solution, the resultant wet gel would replicate the density of the test solution (marked by ρ_0). Afterwards, the saturated wet gel was dropped into a known solvent A (with density of ρ_{A}). Then ρ_0 could be compared with ρ_{A} by simply monitoring if the position of wet gel in solvent A. If the gel floats on the solvent, then we conclude that $\rho_0 < \rho_{\mathrm{A}}$, and vice versa. Then we could quickly dropped this gel into solvent B with density of ρ_{B} ($\rho_{\mathrm{B}} < \rho_{\mathrm{A}}$). If the gel sinks in this case, it means $\rho_{\mathrm{B}} < \rho_0 < \rho_{\mathrm{A}}$. Finally, by dropping the gel in different solvent with known density and monitoring their position in corresponding solvent, the unknown ρ_0 could be limited to a narrow range which is enough for routine requirement.

References:

[s1] L. Chen, B. Wei, C. Li, X. Zhang, *Small* 2014*,* **9**, 2331.

[s2] L. Chen, R. Du, J. Zhu, Y. Mao, C. Xue, N. Zhang, Y. Hou, J. Zhang, T. Yi, *Small* 2015, **11**, 1423.

[s3] L. Chen, C. Xu, R. Du, Y. Mao, C. Xue, L. Chen, L. Qu, J. Zhang, T. Yi, *J. Mater. Chem. A*., 2015, **3**, 5617.

[s4] R. Du, J. Wu, L. Chen, H. Huang, X. Zhang, J. Zhang, *Small* 2014*,* **10**, 1387.

[s5] R. Du , N. Zhang , J. H. Zhu , Y. Wang , C. Y. Xu , Y. Hu , N. N. Mao , H. Xu , W. J. Duan , L. Zhuang , L. T. Qu , Y. L. Hou , J. Zhang, *Small* 2015, DOI: 10.1002/smll.201500587.

[s6] R. Du, Q. Zhao, N. Zhang, J. Zhang, *Small* 2015, DOI: 10.1002/smll.201403170.

[s7] M. Wang, I. V. Anoshkin, A. G. Nasibulin, J. T. Korhonen, J. Seitsonen, J. Pere, E. I. Kauppinen, R. H. A. Ras, O. Ikkala, *Adv. Mater.* 2013*,* **25**, 2428.

[s8] Y. Tao, X. Xie, W. Lv, D. M. Tang, D. Kong, Z. Huang, H. Nishihara, T. Lshii, B. Li, D. Golberg, F. Kang, T. Kyotani, Q. H. Yang, *Sci. Rep.* 2013*,* **3**, 2975.

[s9] A. Lekawa-Raus, J. Patmore, L. Kurzepa, J. Bulmer, K. Koziol, *Adv. Funct. Mater.,* 2014*,* **24**, 3661.

Part III: Figures and Tables

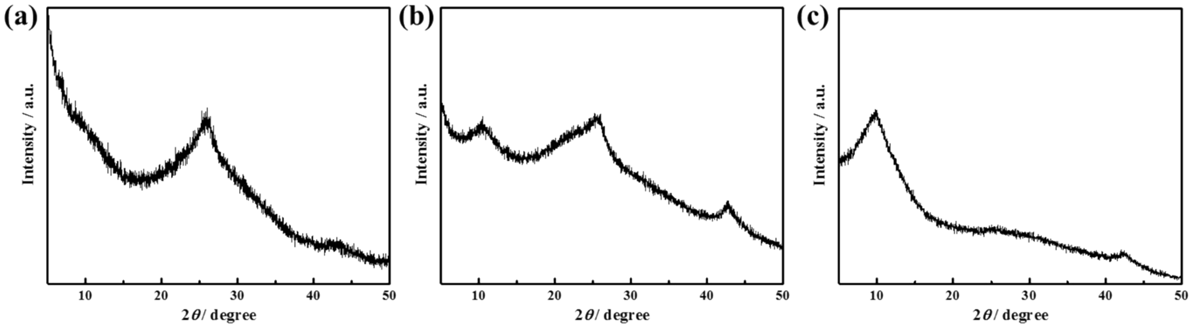

Figure S1. The XRD spectra of oxidized nano-carbon precursors. (a) ox-MWNTs, (b) CNTs@ GONRs, and (c) GONRs.

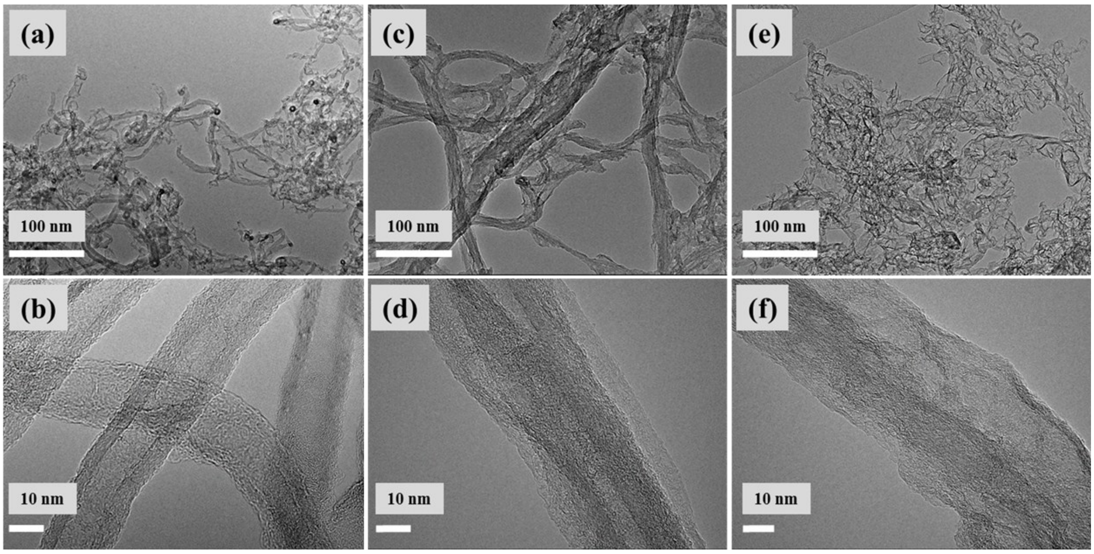

Figure S2. The TEM images of aerogels after pyrolysis at 1030 °C. (a-b) MWNTs aerogel, (c-d) CNTs@GNRs aerogel, and (e-f) GNRs aerogel.

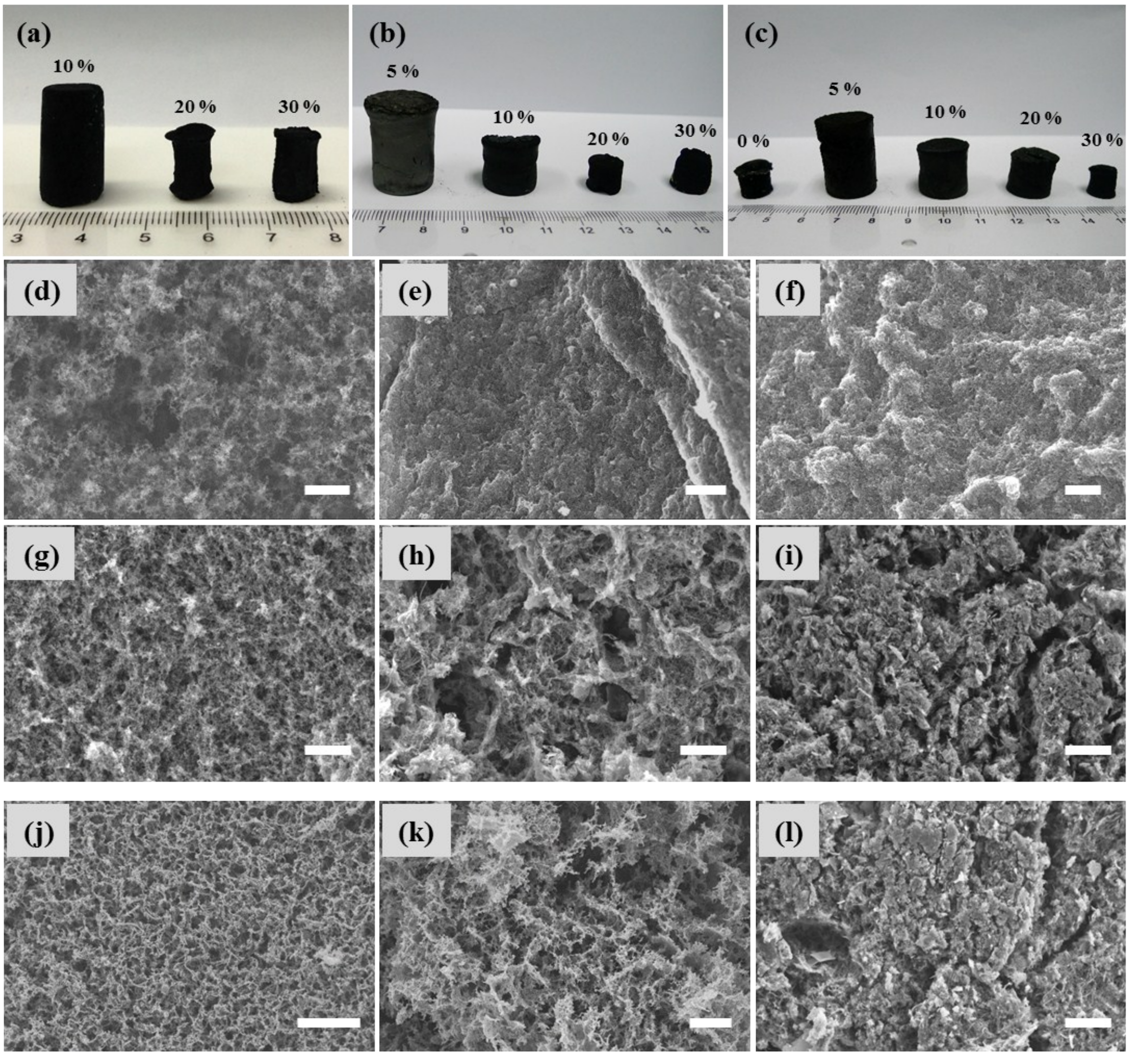

Figure S3. The digital photos of (a) MWNTs aerogel, (b) CNTs@GNRs aerogel, and (c) GNRs aerogels prepared with different pyrrole concentrations. Corresponding SEM images, (d-f) showed the MWNTs aerogel prepared with 10, 20, and 30 vol% pyrrole, respectively; (g-i) showed the CNTs@GNRs aerogel prepared with 10, 20, and 30 vol% pyrrole, respectively; (j-l) showed the GNRs aerogel prepared with 0, 5, and 30 vol% pyrrole, respectively. The concentration of all the carbon precursors were fixed at 5 mg mL^{-1}. The scale bar of SEM images is 3 μm.

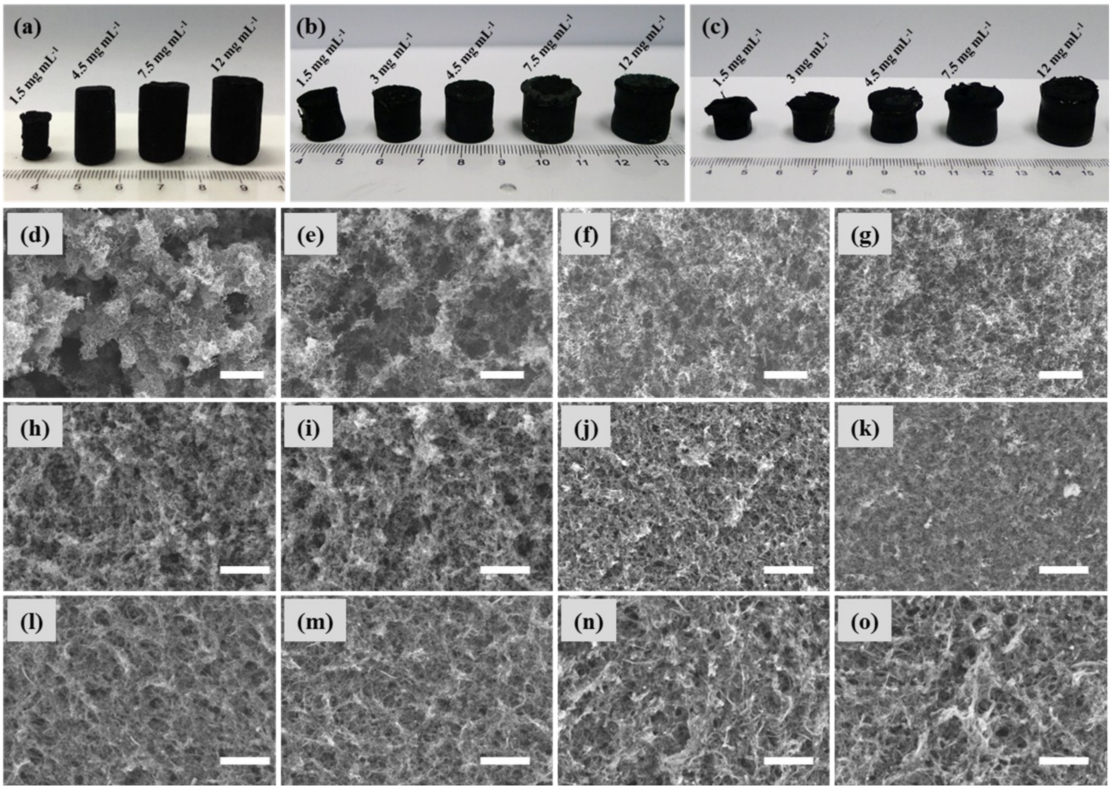

Figure S4. The digital photos of (a) MWNTs aerogel, (b) CNTs@GNRs aerogel, and (c) GNRs aerogel prepared with different initial carbon precursor concentrations. Corresponding SEM images, (d-g) showed the CNTs aerogel prepared with 1.5, 4.5, 7.5, 12 mg mL^{-1} ox-MWNTs, respectively; (h-k) showed the CNTs@GNRs aerogel prepared with 1.5, 4.5, 7.5, 12 mg mL^{-1} CNTs@GONRs, respectively; (l-o) showed the GNRs aerogel prepared with 1.5, 4.5, 7.5, 12 mg mL^{-1} GONRs, respectively. All the samples were prepared with 10 vol% pyrrole. The scale bar of SEM images is 2 μm.

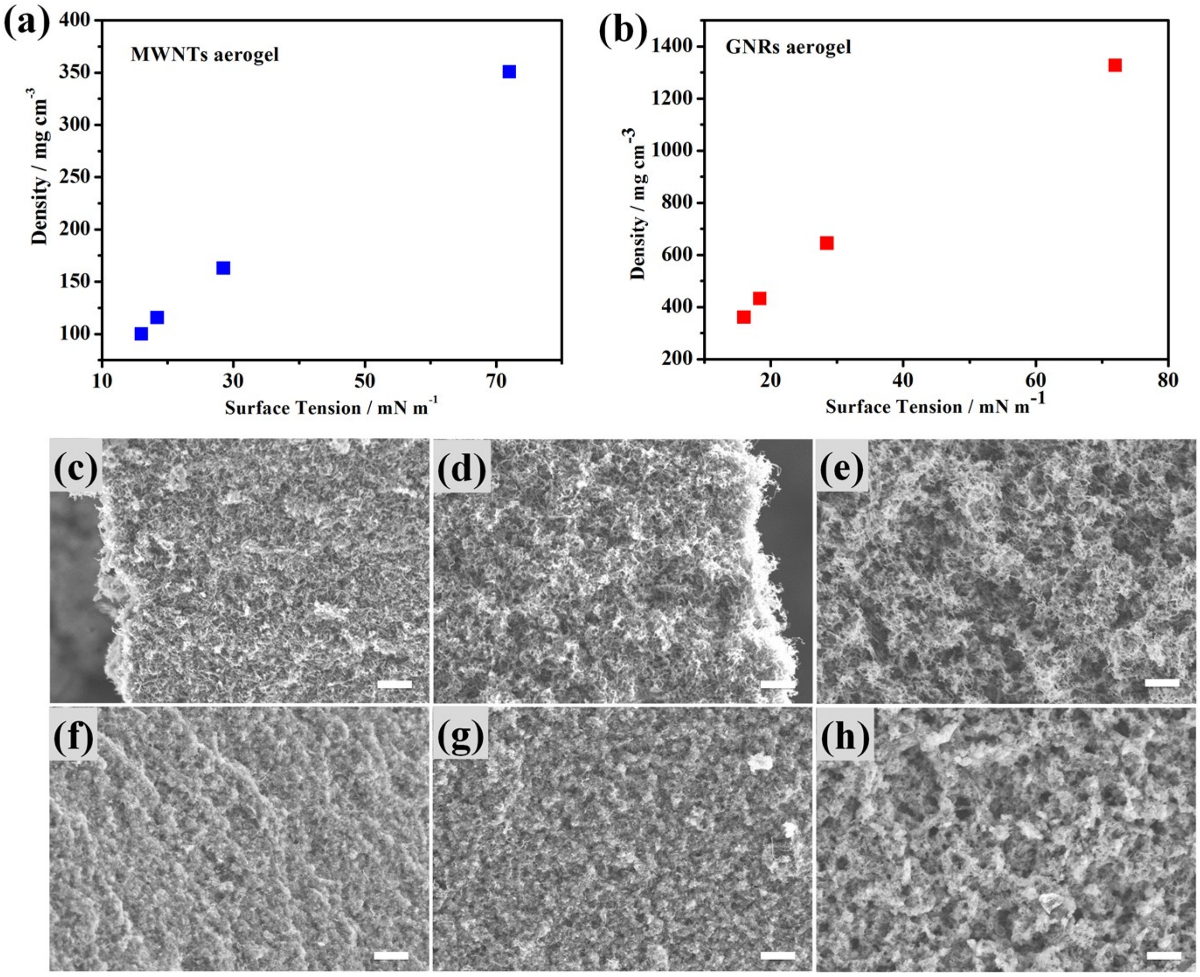

Figure S5. The density evolution of (a) CNTs and (b) GNRs with different surface tension of solvents. The samples were dried in heat-drying mode. Corresponding SEM images, (c-e) showed the CNTs aerogel from solvents of water, toluene and n-pentane, respectively. (f-h) showed the GNRs aerogel from solvents of water, toluene and n-pentane, respectively. The aerogel samples were prepared with 5 mg mL^{-1} carbon precursors (ox-MWNTs and GONRs) and 10 vol% pyrrole. The scale bar of SEM images is 1 μm.

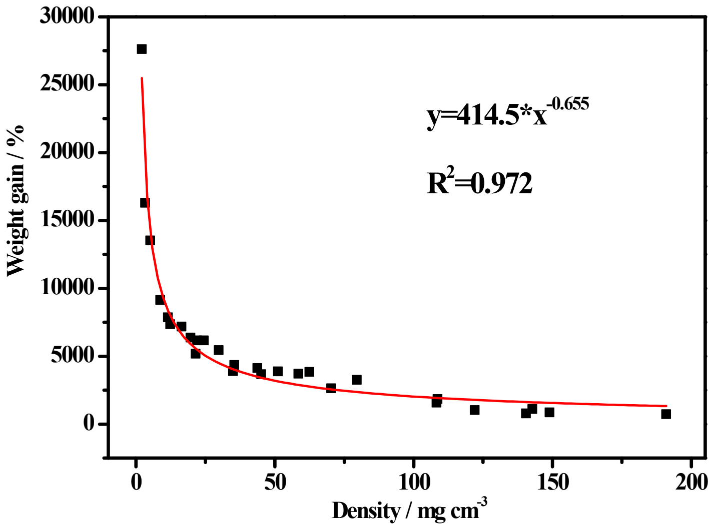

Figure S6. Fitting of the weight gain *vs.* density of aerogels. The data points are well fitted by a power function. The bromobenzene was used as adsorbate.

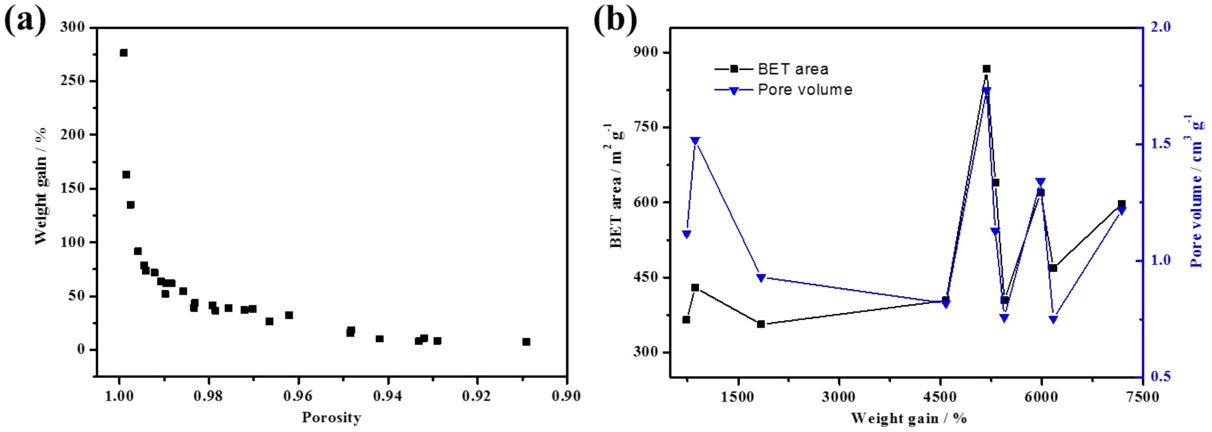

Figure S7. (a) The relationship of weight gain *vs.* porosity of aerogels. (b) The relationship of BET surface area and pore volume (V_{BJH}: calculated by BJH desorption method) *vs.* weight gain. The bromobenzene was used as adsorbate.

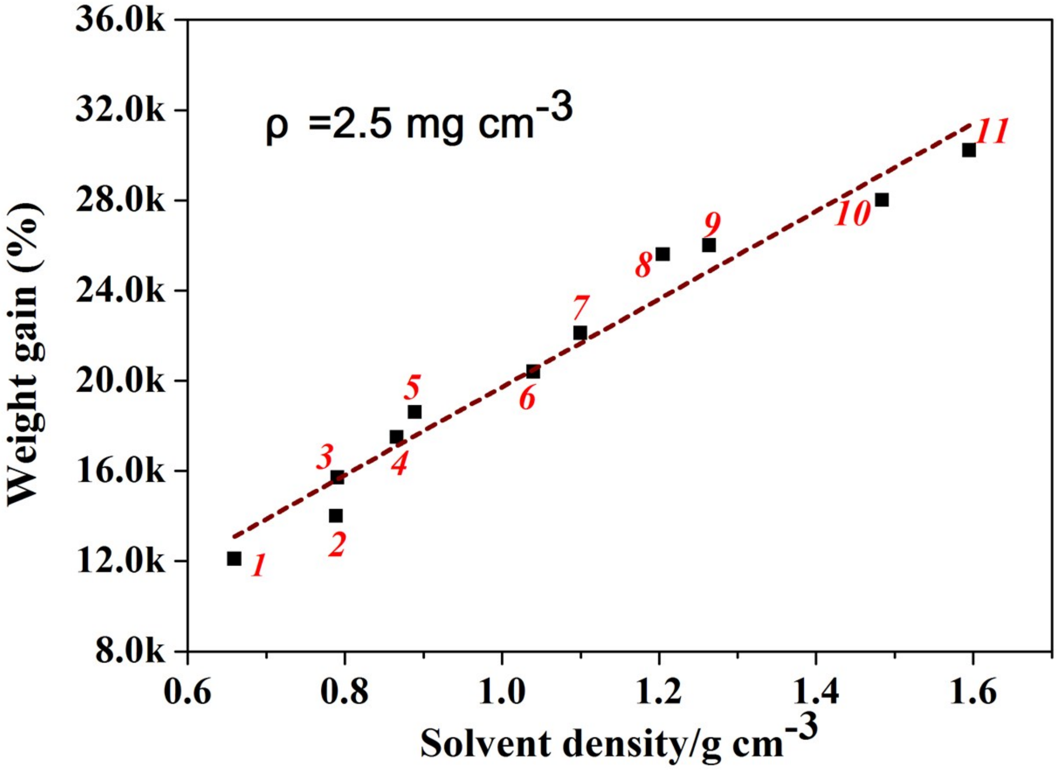

Figure S8. Absorption capacities (Q) of the PDMS modified aerogel (pristine aerogel ρ = 2.5 mg cm^{-3}) for a range of organic solvents in terms of their densities (ρ). The numbers (**1-11**) represent *n*-hexane, ethanol, methanol, toluene, THF, phemethylol, DMSO, nitrobenzene, glycerinum, chloroform and phenixin, respectively.

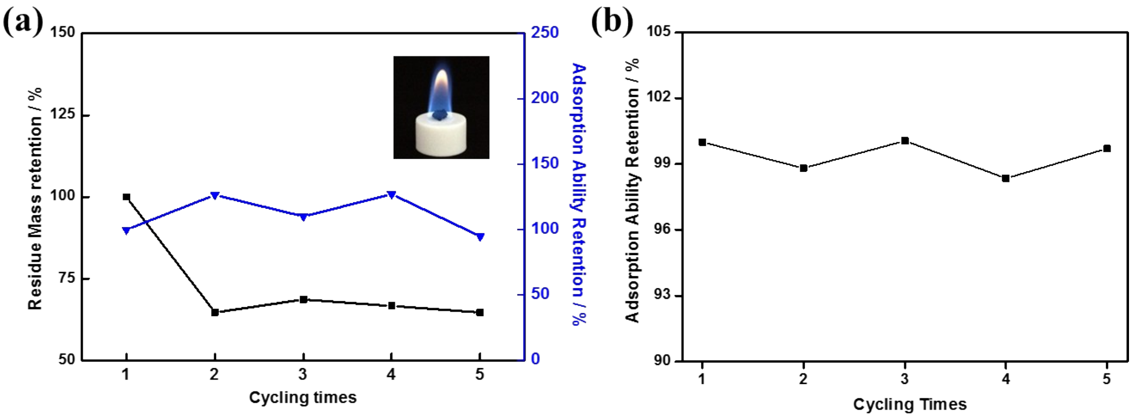

Figure S9. (a) The residue mass and adsorption capacity retention of MWNTs aerogel after regeneration by burning. (b) The adsorption capacity retention of MWNTs aerogel after regeneration by heating.

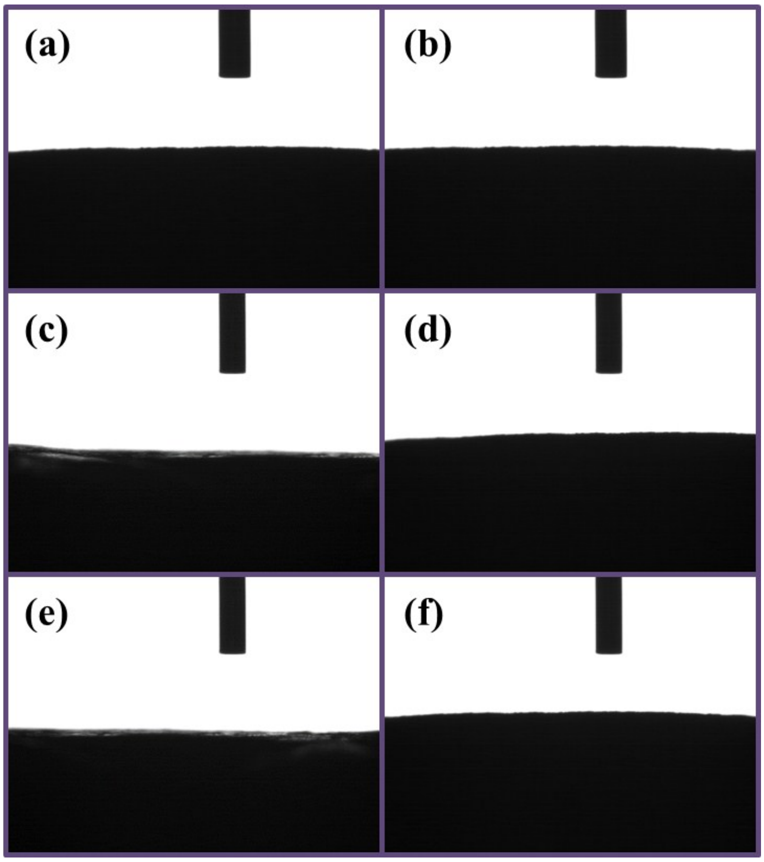

Figure S10. The contact angle of the (a) freshly prepared MWNTs aerogel, (b) MWNTs aerogel, (c) GNRs aerogel, (d) CNTs@GNRs aerogel, (e) pure graphene aerogel, and (f) graphene/pyrrole aerogel. (b-f) were post pyrolyzed at 1030 °C for 3 hours under argon atmosphere.

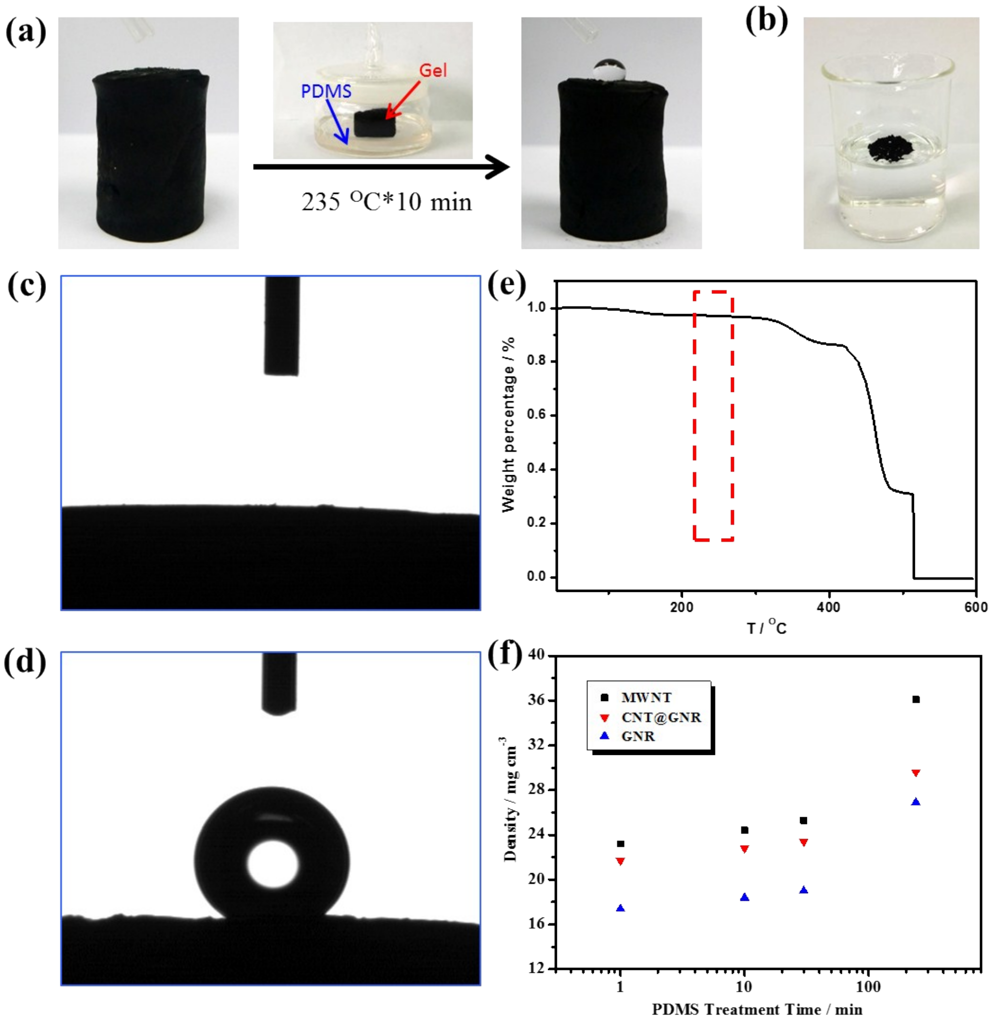

Figure S11. (a) Demonstration of modification process of GNRs aerogel by co-heating with PDMS. (b) The modified aerogel could float on the water even after grinding to the powder, indicating that both external surface and inside of aerogel was highly hydrophobic after PDMS modification. Contact angle of GNRs aerogel pyrolyzed at 1030 °C (c) before and (d) after polydimethylsiloxane (PDMS) modification. (e) TG curve of PDMS in the air which shows only slight weight loss observed around 235 °C, representing vaporation of short-chain PDMS with low molecular weight. (f) The density evolution of MWNTs, CNTs@GNRs, and GNRs aerogels with increasing PDMS treatment time.

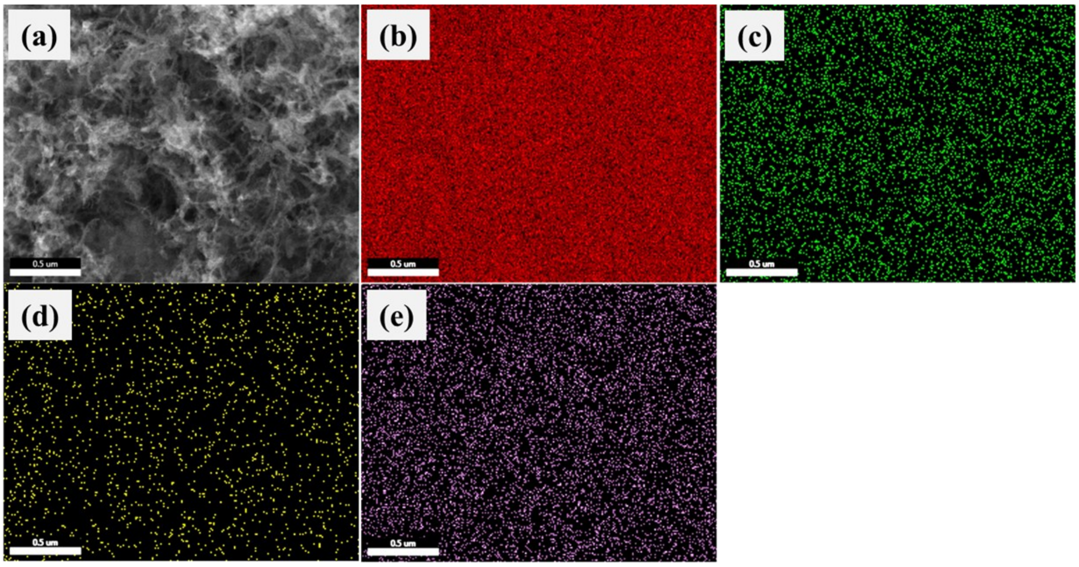

(f)

Element	C	N	O	Si
Atom %	92.78	4.03	2.59	0.6

Figure S12. The (a) SEM images and corresponding elemental mapping of (b) carbon, (c) nitrogen, (d) oxygen, and (e) silicon of a PDMS-modified MWNTs aerogel which was pre-pyrolyzed at 750 °C. (f) The corresponding elemental composition given by EDX spectra.

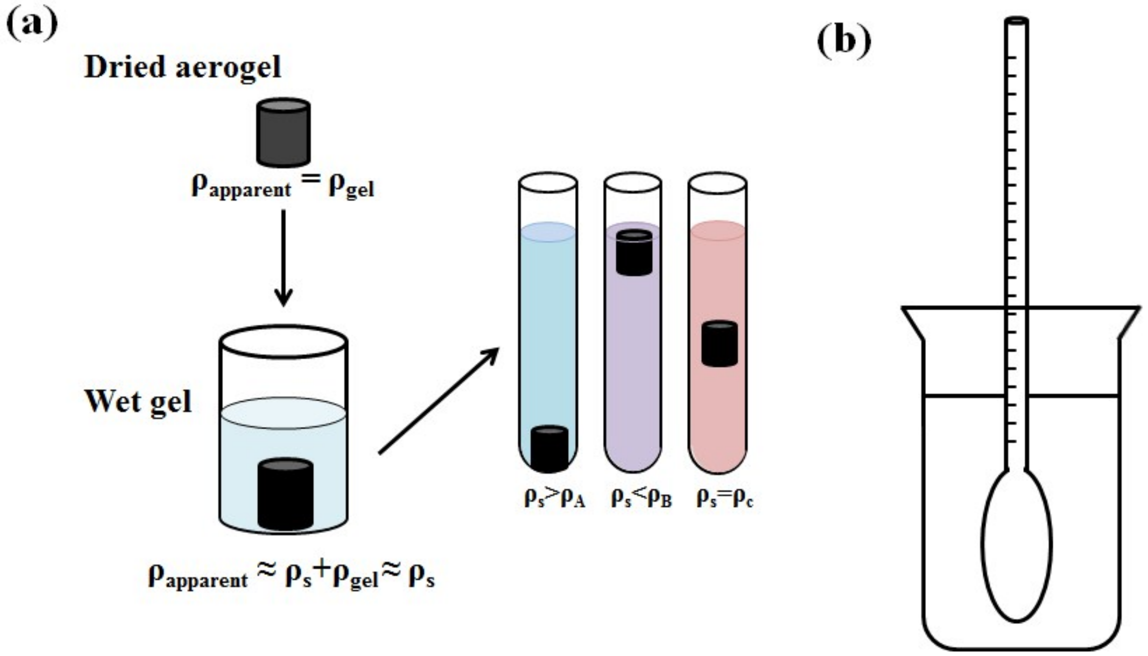

Figure S13. The demonstration of (a) our strategy (aerogel-based densitometers) and (b) traditional strategy (glass-made floating-type densitometers) for measurement of liquid density.

Traditionally, glass-made float-type densitometers with accurate shape were always employed to measure the density. The densitometer was pre-calibrated by various standard liquid to acquire the graduation on the device. It should be noted that in order to obtain high accuracy, densitometers with length more than 20 cm were often used to make it easy to read the graduation. For an unknown solution, the density was measured by inserting the densitometer with appropriate measure range into solution and reading the graduation. Although the accuracy was high (ca. 0.001 g mL^{-1}), the measurable density range was quite narrow (0.1 g mL^{-1}). Moreover, a large quantity of test solution was required to adapt the large size of the densitometer.

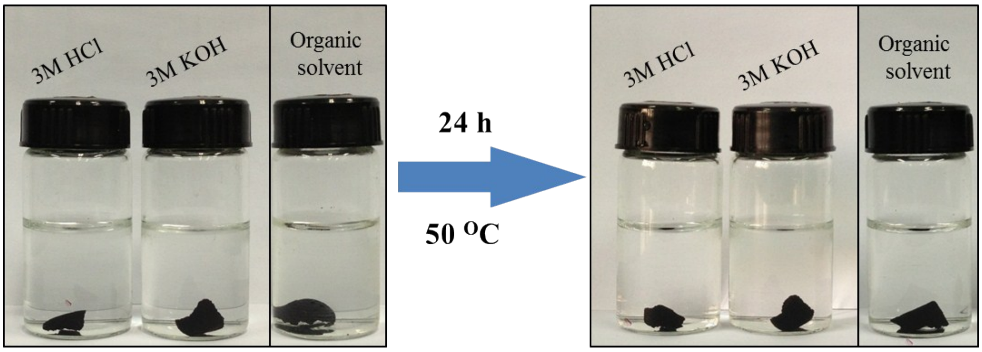

Figure S14. The demonstration of solvent resistance of MWNTs aerogel by subjecting the aerogel into various solvents, and no change was observed after treatment with 24 hours under 50 ºC.

Table S1. Oil uptake capacity of various adsorbents.

Absorbent	Oil	Adsorption capacity g g^{-1}	Reference
N-doped MWNTs, GNRs and CNTs@GNRs aerogels	Hexane, ethanol, toluene, DMSO, chloroform, nitrobenzene, phenoxin, bromobenzene, etc.	Up to 302, tunable	This work
Boron-doped MWNT sponges	Ethanol, toluene, chloroform, engine oil, etc.	20~130	1
CNT sponges	Ethanol, Hexane, DMF, Ethylene, glycol, Chloroform, Gasoline	80~180	2
Carbon nanofiber aerogels	Phenoxin Cyclohexane, Vegetable oil, Gasoline, etc.	40~115	3
Carbon nanofiber aerogels	Ethanol, acetone, chloroform, gasoline, etc.	50~140	4
Carbon nanofiber aerogels	Methanol, ethanol, phenoxin, ether, diesel oil, gasoline, etc.	106-312	5
Twisted carbon fiber aerogel	Ethanol, cyclohexane, toluene, chloroform, pump oil, etc.	50~192	6
Carbon Microbelt Aerogel	Chloroform, hexane, DMF, olive oil, etc.	56-188	7
Melamine-formaldehyde sponges	n-hexane, DMSO, toluene, soybean oil, pump oil, etc.	79-195	8
Spongy graphene	Methanol, THF, DMSO, Toluene, Pump oil, Nitrobenzene, chloroform, etc.	20~86	9
Graphene/a-FeOOH composite aerogels	cyclohexane, toluene, vegetable oil, etc.	10~30	10
N-doped graphene aerogels	Ethanol, acetone, chloroform,	200~600	11

	gasoline, etc.		
Reduced graphite oxide foams	Cyclohexane, chlorobenzene, toluene, petroleum, motor oil	5~40	12
Graphene aerogels	Ethanol, toluene, hexane, phenoxin, pump oil, etc.	15~60	13
Graphene-CNT hybrid foams	DMF, toluene, chloroform, compressor oil, etc.	80~130	14
Graphene-CNT hybrid aerogels	Ethanol, toluene, n-hexane, chloroform, motor oil, etc.	215~913	15
Graphene/polyvinylidene fluoride aerogels	Ethanol, THF, toluene, chloroform, pump oil, etc.	15~80	16
Porous boron nitride nanosheets	Ethanol, toluene, pump oil, engine oil, ethylene glycol	19~35	17
Nanowire membrane	oils and some organic solvents	4~20	18
Graphene sponges	Ethanol, vegetable oil, diesel oil, chloroform, heptane, etc.	60-160	19
Polyurethane based sponges	Octane, decane, dodecane, lubricating oil	13~20	20
Polyurethane/ iron oxide nanoparticles/polytrtrafluoroethylene foams	Mineral oil	~13	21
Activated carbon	benzene, toluene	<1	22
Nanoporous polydivinylbenzene	n-heptane, benzene	8~16	23
Conjugated microporous polymers	Hexane, DMF, ethanol, nitrobenzene, chloroform, toluene, pump oil, etc.	6~33	24

Table S2. Densities comparison of different aerogels.

Materials	**Density / mg cm^{-3}**	**Reference**
N-doped MWNTs, GNRs and CNTs@GNRs aerogels	2.5~1327, tunable	This work
Ultralight graphene-CNT hybrid aerogels	0.16	15
3D graphene frameworks	2.1±0.3	11
Ultralight graphene aerogel	3~5	25
MWNT aerogels	4	2
Carbon nanofiber aerogels	4~6	4
Graphene foams	5	26
Graphene/CNT foams	6.9	27
CNT aerogels	~7.5	28
Graphene aerogels	4.4~7.9	29
Carbon nanofiber aerogels	10	4
CNT sponges	5~10	2
Graphene aerogels	10	30
Sponge graphene	12±5	9
3D graphene	~30	31
Nitrogen-doped MWNT sponges	30~55	32
3D Graphene	16~25	33
Carbonaceous aerogels	58~1050	34

Table S3. Comparison of commercial glass-made densitometers and aerogel densitometers proposed in our work.

	Commercial densitometer	**Aerogel densitometer**
Measuring range	0.1 g mL^{-1}	Arbitrary
Required solution amount	Large	Very Small
Device shape and size	Regular shape, Several tens centimeters long	Arbitrary
Solution type	No limitation	No limitation
Stability	Stable	Stable
Accuracy	0.001 g mL^{-1}	~0.006 g mL^{-1} in our case

References:

[1] D. P. Hashim, N. T. Narayanan, J. M. Romo-Herrera, D. A. Cullen, M. G. Hahm, P. Lezzi, J. R. Suttle, D. Kelkhoff, E. Munoz-Sandoval, S. Ganguli, *Sci. Rep.* 2012, **2**, 363.

[2] X. Gui, J. Wei, K. Wang, A. Cao, H. Zhu, Y. Jia, Q. Shu, D. Wu, *Adv. Mater.* 2010, **22**, 617.

[3] H. W. Liang, Q. F. Guan, L. F. Chen, Z. Zhu, W. J. Zhang, S. H. Yu, *Angew. Chem. Int. Ed.* 2012, **51**, 5101.

[4] Z.-Y. Wu, C. Li, H.-W. Liang, Y.-N. Zhang, X. Wang, J.-F. Chen, S.-H. Yu, *Sci. Rep.* 2014, **4**, 4079.

[5] Z. Y. Wu , C. Li , H. W. Liang , J. F. Chen , S. H. Yu , *Angew. Chem. Int. Ed.* 2013, **52**, 2925.

[6] H. C. Bi , Z. Y. Yin , X. H. Cao , X. Xie , C. L. Tan , X. Huang , B. Chen , F. T. Chen , Q. L. Yang , X. Y. Bu , X. H. Lu , L. T. Sun , H. Zhang , *Adv. Mater.* 2013, **25**, 5916.

[7] H. C. Bi, X. Huang, X. Wu, X. Cao, C. L Tan, Z. Yin, X. Lu, L. Sun, H. Zhang, *Small,* 2014, **10**, 3544-3550.

[8] C. Ruan, K. Ai, X. Li, L. Lu. *Angew. Chem. Int. Ed.* 2014*,* **53**, 1.

[9] H. Bi, X. Xie, K. Yin, Y. Zhou, S. Wan, L. He, F. Xu, F. Banhart, L. Sun, R. S. Ruoff, *Adv. Funct. Mater.* 2012, **22**, 4421.

[10] H.-P. Cong, X.-C. Ren, P. Wang, S.-H. Yu, *ACS nano* 2012, **6**, 2693.

[11] Y. Zhao, C. Hu, Y. Hu, H. Cheng, G. Shi, L. Qu, *Angew. Chem. Int. Ed.* 2012*,* **51**, 11371.

[12] Z. Niu, J. Chen, H. H. Hng, J. Ma, X. Chen, *Adv. Mater.* 2012*,* **24**, 4144.

[13] J. Wang, Z. Shi, J. Fan, Y. Ge, J. Yin, G. Hu, *J. Mater. Chem.* 2012, **22**, 22459.

[14] X. Dong, J. Chen, Y. Ma, J. Wang, M. B. Chan-Park, X. Liu, L. Wang, W. Huang, P. Chen, *Chem. Commun.* 2012, **48**, 10660.

[15] H. Y. Sun, Z. Xu, C. Gao. *Adv. Mater.* 2013*,* **25**, 2554.

[16] R. Li, C. Chen, J. Li, L. Xu, G. Xiao, D. Yan, *J. Mater. Chem. A* 2014, **2**, 3057.

[17] W. Lei, D. Portehault, D. Liu, S. Qin, Y. Chen, *Nat. Commun.* 2013, **4**, 1777.

[18] J. Yuan, X. Liu, O. Akbulut, J. Hu, S. L. Suib, J. Kong, F. Stellacci, *Nat. Nanotech.* 2008, **3**, 332.

[19] J. Zhao, W. Ren, H. M. Cheng, *J. Mater. Chem.* 2012*,* **22**, 20197.

[20] Q. Zhu, Q. Pan, F. Liu, *J. Phys. Chem. C* 2011, **115**, 17464.

[21] P. Calcagnile, D. Fragouli, I. S. Bayer, G. C. Anyfantis, L. Martiradonna, P. D. Cozzoli, R. Cingolani, A. Athanassiou, *ACS nano* 2012, **6**, 5413.

[22] M. Lillo-Ródenas, D. Cazorla-Amorós, A. Linares-Solano, *Carbon* 2005, **43**, 1758.

[23] Y. Zhang, S. Wei, F. Liu, Y. Du, S. Liu, Y. Ji, T. Yokoi, T. Tatsumi, F.-S. Xiao, *Nano Today* 2009, **4**, 135.

[24] A. Li, H.-X. Sun, D.-Z. Tan, W.-J. Fan, S.-H. Wen, X.-J. Qing, G.-X. Li, S.-Y. Li, W.-Q. Deng, *Energy Environ. Sci.* 2011, **4**, 2062.

[25] H. Hu, Z. Zhao, W. Wan, Y. Gogotsi, J. Qiu, *Adv. Mater.* 2013*,* **25**, 2219.

[26] Z. P. Chen, W. C. Ren, L. B. Gao, B. L. Liu, S. F. Pei, H. M. Cheng, *Nat. Mater.* 2011*,* **10**, 424.

[27] X. C. Dong, J. Chen, Y. W. Ma, J. Wang, M. B. Chan-Park, X. M. Liu, L. H. Wang, W. Huang, P. Chen, *Chem. Commun.* 2012*,* **48**, 10660.

[28] M. B. Bryning, D. E. Milkie, M. F. Islam, L. A. Hough, J. M. Kikkawa, A. G. Yodh, *Adv. Mater.* 2007*,* **19**, 661.

[29] J. Li, J. Li, H. Meng, S. Xie, B. Zhang, L. Li, H. Ma, J. Zhang, M. Yu, *J. Mater. Chem. A,* 2014*,* **2**, 2934.

[30] M. A. Worsley, P. J. Pauzauskie, T. Y. Olson, J. Biener, J. H. Satcher, Jr., T. F. Baumann, *J. Am. Chem. Soc.* 2010*,* **132**, 14067.

[31] Z. H. Tang, S. L. Shen, J. Zhuang, X. Wang, *Angew. Chem. Int. Ed.* 2010*,* **49**, 4603.

[32] C. Shan, W. Zhao, X. Lu, D. J. O'Brien, Y. Li, Z. Cao, A. L. Elias, R. Cruz-Silva, M. Terrones, B. Wei, J. Suhr, *Nano Lett.* 2013*,* **13**, 5514.

[33] M. A. Worsley, T. Y. Olson, J. R. I. Lee, T. M. Willey, M. H. Nielsen, S. K. Roberts, P. J. Pauzauskie, J. Biener, J. H. Satcher, Jr., T. F. Baumann, *J. Phys. Chem. Lett.* 2011*,* **2**, 921.

[34] X. L. Wu, T. Wen, H. L. Guo, S. B. Yang, X. K. Wang, A. W. Xu, *ACS Nano,* 2013*,* **7**, 3589.